



Cite this: *Catal. Sci. Technol.*, 2020, **10**, 2961

## Investigation on the simultaneous removal of COS, CS<sub>2</sub> and O<sub>2</sub> from coke oven gas by hydrogenation on a Pd/Al<sub>2</sub>O<sub>3</sub> catalyst

Eva Kamp,<sup>a</sup> Holger Thielert,<sup>b</sup> Olaf von Morstein,<sup>b</sup> Sven Kureti,<sup>c</sup> Norman Schreiter<sup>c</sup> and Jens-Uwe Repke   <sup>\*a</sup>

The present study deals with the processing of coke oven gas mainly composed of H<sub>2</sub>, CH<sub>4</sub>, N<sub>2</sub> and CO to provide a feedstock for the synthesis of base chemicals. In this respect, the particular focus of this work is the simultaneous reduction of critical trace components like COS, CS<sub>2</sub> and O<sub>2</sub> by catalytic reaction with H<sub>2</sub>. The investigations were performed in synthetic coke oven exhaust using a Pd/Al<sub>2</sub>O<sub>3</sub> catalyst. The results of the hydrogenation tests showed complete conversion of COS, CS<sub>2</sub> and O<sub>2</sub> at 200 °C and above with selective formation of H<sub>2</sub>S. However, below 200 °C the conversion of O<sub>2</sub> was markedly reduced and CH<sub>3</sub>-SH appeared as a by-product. Mechanistic studies were performed by *in situ* diffuse reflectance infrared Fourier transform spectroscopy coupled with mass spectrometry. These investigations demonstrated dissociative adsorption of COS on the catalyst at 150 °C resulting in the formation of bridged CO adsorbates and probably elemental sulfur. It is assumed that these species predominate the active Pd surface under reaction conditions. Consequently, the adsorption of O<sub>2</sub> and the reaction to H<sub>2</sub>O is suppressed thus substantiating the decrease in performance at low temperatures. However, increasing the temperature to 200 °C and above leads to desorption of CO and sulfur compounds restoring the efficiency of the catalyst.

Received 23rd December 2019,  
Accepted 3rd April 2020

DOI: 10.1039/c9cy02579k

rsc.li/catalysis

## 1. Introduction

Deep desulfurization is widely used for the removal of sulfur from natural gas as well as refined petroleum products, for instance gasoline and diesel fuels. The reduction of sulfur is primarily required to avoid poisoning of downstream processes such as fuel cells or depollution catalysts of combustion engines. Although well-established in petrochemical industry, deep desulfurization is still a matter of R&D, particularly to meet future legislative regulations addressing the sulfur fraction of fuels.<sup>1–6</sup> Additionally, the reduction of sulfur is also considered for coke oven gases aiming sulfur contents below 10 mol ppm, whereas up to now no cost-efficient process exists. Coke oven gas is a by-product of the steel production and mainly consists of 60 vol% H<sub>2</sub>, 20 vol% CH<sub>4</sub> and 6 vol% CO. Thus, the exhaust of coke ovens shows promising potential as a feedstock for basic chemicals, *e.g.* methanol.<sup>7</sup> However, the exhaust also contains critical

sulfur components such as COS, CS<sub>2</sub> and mercaptans representing strong catalyst poisons, especially for Ni and Cu catalysts used in steam reforming and methanol synthesis, respectively.<sup>7,8</sup> Therefore, deep desulfurization is required, which is mostly realized by hydrodesulfurization (HDS). HDS implies hydrogenolysis of organosulfur compounds on CoMo or NiMo catalysts yielding sulfur-free hydrocarbons and H<sub>2</sub>S. The H<sub>2</sub>S produced can subsequently be removed by ZnO adsorbents or scrubbing processes.<sup>9–11</sup> As a result, HDS leads to drastic decrease in sulfur proportions down to 15–30 mass ppm as required for ultra-low sulfur fuels for instance.<sup>12</sup>

Furthermore, for deep desulfurization of diesel fuels, noble metal catalysts based on platinum and palladium were investigated with promising results.<sup>13–17</sup> But, only little is known on the HDS performance of noble metals in gaseous streams containing COS or mercaptans. Additionally, noble metals provide advantageous features, which are relevant for their use in gas oven exhaust, such as (i) enhancement of the removal of oxygen by reaction with hydrogen to water, since it can be harmful in downstream processes (*e.g.* due to safety issues or corrosion effects), (ii) suppression of coke formation by hydrogenation of olefins and (iii) their superior HDS activity as referred to traditional CoMo catalysts.<sup>14</sup> However, there is a debate in the literature on the stability of noble metal catalysts towards sulfur poisoning.<sup>13–18</sup> In this respect,

<sup>a</sup> TU Berlin, Process Dynamics and Operations Group, Strasse des 17. Juni 13, Berlin 10623, Germany. E-mail: jens-uwe.repke@tu-berlin.de

<sup>b</sup> Thyssenkrupp Industrial Solutions AG, Friedrich-Uhde-Strasse 15, Dortmund 44141, Germany

<sup>c</sup> TU Bergakademie Freiberg, Institute of Energy Process Engineering and Chemical Engineering Institut, chair of Reaction Engineering, Freiberg 09599, Germany



some papers investigated the interaction of sulfur compounds with Pt and Pd catalysts. Bartholomew *et al.*<sup>19</sup> reported on the dissociative adsorption of COS, CS<sub>2</sub> and methyl mercaptan (CH<sub>3</sub>SH) with strong sticking of the sulfur on the noble metals. Moreover, Reinhoudt *et al.*<sup>14</sup> studied the nature of the active sites on alumina–silica-supported Pt suggesting that the desulfurization takes place on vacancies present in small platinum particles. High activity was also attributed to the support acidity affecting the electron deficiency and weakening the noble metal–sulfur bond.<sup>20</sup> Additionally, Pt and Pd sulfides originated from HDS can effectively be regenerated by reaction with H<sub>2</sub> above 463 K.<sup>17,21,22</sup>

With the above background the present study is the first that deals with the simultaneous removal of organosulfur compounds and O<sub>2</sub> from coke oven gas by hydrogenation on a commercially available Pd/Al<sub>2</sub>O<sub>3</sub> catalyst. The investigations were made in a synthetic exhaust using a laboratory test bench with fixed bed reactor. COS and CS<sub>2</sub> were taken as model components showing highest importance among the sulfur species in practice.<sup>20</sup> In addition to the evaluation of the catalytic performance, *in situ* diffuse reflectance infrared Fourier transform spectroscopy coupled with mass spectrometry was conducted to obtain some mechanistic insights into the complex reaction network, particularly at low temperatures.

## 2. Experimental

### 2.1. Catalytic studies

The performance of the commercial Pd/Al<sub>2</sub>O<sub>3</sub> catalyst towards hydrogenation of COS and CS<sub>2</sub> combined with reduction of O<sub>2</sub> was studied in a coke oven model exhaust by employing a laboratory bench equipped with fixed bed reactor. The catalyst implied a Pd load of 0.3 wt% and was used in form of spheres with a diameter of 3 mm. According to Mears and Weisz–Prater criteria it was deduced that neither film nor pore diffusion limit the chemical kinetics.<sup>23</sup> The sample (68.6 g) was fixed in the stainless steel tube reactor (i.d. 30 mm) by quartz wool and a sieve resulting in a bed height of 15 cm. In front of the packed bed, glass beads (2.85–3.45 mm, Carl Roth) were placed to improve heating of the inlet gas. The temperature was recorded by two Pt100 shunts (type 27-7125, Bartec) directly located in front of and behind the catalyst bed. The catalyst was initially pre-treated at 350 °C for 1 h with 50% H<sub>2</sub> in N<sub>2</sub>. Before the tests, the sample was heated up in N<sub>2</sub> flow (5.2 LN/min) to the specific test temperature and then the feed was adjusted until steady state conditions were reached. Each test point was held for 90 min. After this, temperature (120–400 °C) or feed composition was varied. The model feed consisted of 60–120 mol ppm COS, 55–120 mol ppm CS<sub>2</sub>, 50 vol% H<sub>2</sub>, 20 vol% CH<sub>4</sub>, 1 vol% O<sub>2</sub> and N<sub>2</sub> as balance. The reactor pressure was regulated with a needle valve behind the reactor to 1.2 bara, whereas the total gas flow was kept at 5.2 LN/min corresponding to a space velocity of 3000 h<sup>-1</sup>. All gases were purchased from Linde. Pure H<sub>2</sub>

(5.0), CH<sub>4</sub> (2.5) and N<sub>2</sub> (5.0) were taken, while the sulfur compounds as well as O<sub>2</sub> were used as mixtures with N<sub>2</sub>. Each volume flow rate was checked by independent mass flow controllers (Brooks Instruments). All electronic devices were controlled by Freelance 2013 software from ABB.

The gas analysis was carried out by gas chromatography (Compact GC 4.0, Global Analyser Solutions) using a pulsed flame photometric detector (PFPD) for COS, CS<sub>2</sub> and H<sub>2</sub>S and a thermal conductivity detector (TCD) for O<sub>2</sub>. Simultaneous measurement of organic sulfur components, H<sub>2</sub>S and O<sub>2</sub> was not possible. Before entering the GC, the gas stream passed a condensate trap to reduce the amount of water in the columns. Furthermore, a pressure regulator was implemented to ensure a constant pressure at the inlet of the GC. With this set-up, reproducible results were achieved.

### 2.2. *In situ* DRIFTS and MS studies

The reaction of COS, O<sub>2</sub> and H<sub>2</sub> on the Pd/Al<sub>2</sub>O<sub>3</sub> catalyst and the bare Al<sub>2</sub>O<sub>3</sub> support was investigated by diffuse reflectance infrared Fourier transform spectroscopy (DRIFTS). The analyses were performed on a FTIR Spectrometer Tensor 27 (Bruker) equipped with MCT detector (Internal) and Praying Mantis DRIFTS optics (Harrick), while gas phase was simultaneously checked by mass spectrometry (Cirrus 2, MKS Instruments). In each experiment, fresh catalyst sample was placed into the cell and was subsequently pre-reduced with a mixture of N<sub>2</sub> and H<sub>2</sub> (50 vol% each) at 300 °C for 15 min following the pre-treatment in the catalytic studies. DRIFTS data were recorded by accumulating 200 scans resulting in a time resolution of *ca.* 5 min. Background spectra were taken at 40 °C and 150 °C and under flowing N<sub>2</sub> (500 mL min<sup>-1</sup>). Subsequently, the sample was exposed to COS (200 mol ppm) at 40 and 150 °C to investigate the resulting adsorbates. For temporal separation of the overall reaction, H<sub>2</sub> and O<sub>2</sub> were successively dosed after the pre-adsorption of COS at 150 °C. Additionally, the simultaneous conversion of the reactive gases was checked at the same temperature by exposing the catalyst and bare support to a mixture of 200 mol ppm COS, 60 vol% H<sub>2</sub>, 1 vol% O<sub>2</sub>. N<sub>2</sub> was used as balance. After the adsorption and reaction steps, the sample was flushed with 500 mL min<sup>-1</sup> N<sub>2</sub> for 25 min to differentiate gas-phase and surface species, while each exposure was made until equilibrium or steady state. The overall gas flow was always kept at 500 mL min<sup>-1</sup>. The DRIFT spectra are presented in form of the Kubelka Munk function defined as  $F(R) = (1 - R)^2/(2R)$ ; R is the quotient of sample and background scans.

## 3. Results and discussion

### 3.1. Conversion of COS, CS<sub>2</sub> and O<sub>2</sub> on Pd/Al<sub>2</sub>O<sub>3</sub> catalyst

At temperatures over 200 °C the conversion of organosulfur compounds (60 mol ppm COS and 55 mol ppm CS<sub>2</sub>) as well as 1 vol% O<sub>2</sub> was complete and stable for the established time on stream of 90 min (Fig. 1). Additionally, the formation of 140 mol ppm H<sub>2</sub>S was observed between 200 and 400 °C, which is the thermodynamically favored product under these



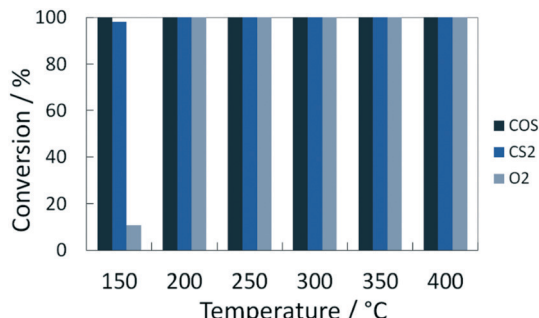
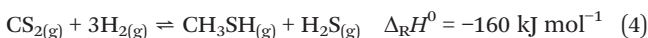
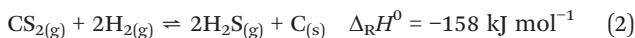
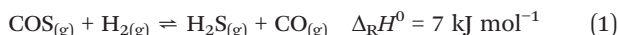


Fig. 1 Stationary conversion of COS, CS<sub>2</sub> and O<sub>2</sub> over temperature in model coke oven gas on Pd/Al<sub>2</sub>O<sub>3</sub> catalyst. Conditions: 3000 1/h, 60 mol ppm COS, 55 mol ppm CS<sub>2</sub>, 1 vol% O<sub>2</sub>, 50 vol% H<sub>2</sub>, 20 vol% CH<sub>4</sub>, N<sub>2</sub> balance.

conditions. This proportion is in line with the stoichiometry of the conversion of COS and CS<sub>2</sub> according to eqn (1) and (2). Note that the discrepancy to the theoretical yield (170 mol ppm) is referred to influence of the condensate trap in front of the GC.



Furthermore, when decreasing the temperature from 200 to 150 °C a strongly unsteady behavior of the catalyst appeared implying continuous decrease of O<sub>2</sub> conversion, which remained almost constant after 200 min at 150 °C (Fig. 2). The analysis of the sulfur components at 150 °C at the end of the experiment showed still high conversion of COS and CS<sub>2</sub>. However, in addition to H<sub>2</sub>S, CH<sub>3</sub>SH was also formed (approx. 30 ppm), whereas both compounds totally amounted to 120 mol ppm (Fig. 3 and Table 1). For CoMo catalysts, Clark *et al.*<sup>24</sup> supposed that CH<sub>3</sub>SH is originated from the hydrogenation of the C-S bond in line with the

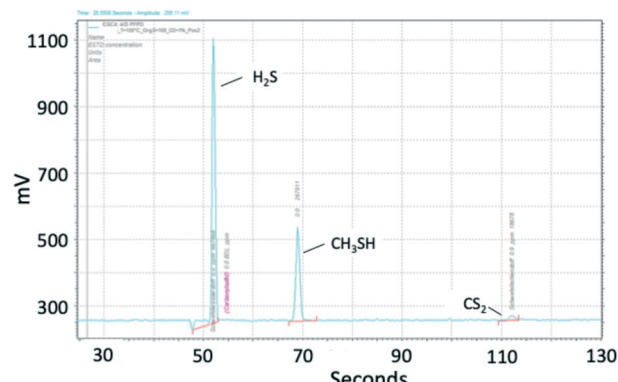


Fig. 3 Chromatogram of sulfur components, measured with PFPD. Conditions: 3000 1/h, 150 °C, 60 mol ppm COS, 55 mol ppm CS<sub>2</sub>, 50 vol% H<sub>2</sub>, 20 vol% CH<sub>4</sub>, 1 vol% O<sub>2</sub>, N<sub>2</sub> balance.

thermodynamics (eqn (4)). Furthermore, it cannot be excluded that some adsorbed sulfur still remained on the catalyst surface<sup>25</sup> and that another sulfur compound was produced, which could not be detected by PFPD. For example, the production of SO<sub>2</sub> is basically feasible when the reaction of S with O<sub>2</sub> is faster than that with H<sub>2</sub>. Other organic sulfur components were not formed, they would have been detected by PFPD.

Moreover, the catalyst was exposed to a model coke oven gas with higher sulfur mole fractions, *i.e.* each 125 mol ppm for COS and CS<sub>2</sub>, to evaluate the effect of sulfur on the catalytic performance. At 200 °C the conversion of O<sub>2</sub> and organic sulfur is complete. Subsequently, the temperature was lowered to 120 °C. This leads to a drop of oxygen conversion below 30% within less than 1 h (Fig. 4). Subsequently, it was heated again to 200 °C resulting in an immediate rise of the conversion to over 95%. Entire removal of O<sub>2</sub> was achieved by further increasing the temperature to 250 °C, whereas COS and CS<sub>2</sub> were also completely converted, *i.e.* the same performance was obtained than before (Fig. 2). Measuring the concentration of the sulfur components at the outlet showed the initially measured full conversions and solely a H<sub>2</sub>S peak in the product stream; note that quantitative detection of H<sub>2</sub>S was not available. This shows that sulfur, which inhibits the O<sub>2</sub> conversion below 150 °C, is released from the catalyst and therefore it can be regenerated by an increase of temperature.

Since the conversion of O<sub>2</sub> to H<sub>2</sub>O is inhibited below 150 °C, while the sulfur compounds are still efficiently converted (<3 ppm), it can be concluded that COS, CS<sub>2</sub> and H<sub>2</sub> predominately chemisorb on the active sites of the catalyst. Furthermore, the higher fractions of the sulfur components obviously favor their adsorption as indicated by the stronger inhibition of the O<sub>2</sub> conversion (Fig. 4). This conclusion is in line with Bartholomew *et al.*,<sup>19</sup> who also observed preferential adsorption of sulfur compounds compared to O<sub>2</sub>. Additionally, it is well known in the literature that sulfur forms strong bonds with metals of group 10 (Ni, Pd, Pt) due to unshared electrons. Therefore, it is assumed that in an

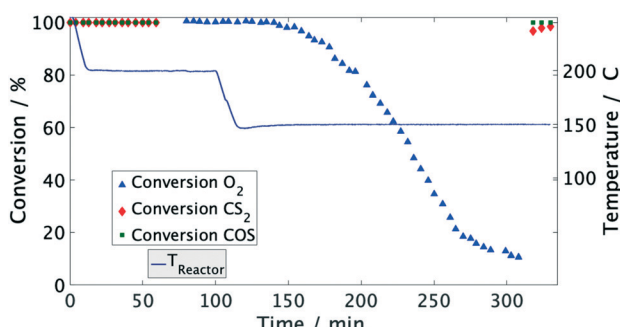


Fig. 2 Conversion of COS, CS<sub>2</sub> and O<sub>2</sub> over time in model coke oven gas on Pd/Al<sub>2</sub>O<sub>3</sub> catalyst. Conditions: 3000 1/h, 60 mol ppm COS, 55 mol ppm CS<sub>2</sub>, 50 vol% H<sub>2</sub>, 20 vol% CH<sub>4</sub>, 1 vol% O<sub>2</sub>, N<sub>2</sub> balance.



**Table 1** Conversion of COS, CS<sub>2</sub>, CH<sub>3</sub>SH and O<sub>2</sub> at steady-state at 200 °C and at 150 °C after 200 min. Conditions: 3000 1/h, 60 mol ppm COS, 55 mol ppm CS<sub>2</sub>, 50 vol% H<sub>2</sub>, 20 vol% CH<sub>4</sub>, 1 vol% O<sub>2</sub>, N<sub>2</sub> balance

	X(COS) in %	X(CS <sub>2</sub> ) in %	y(CH <sub>3</sub> SH) in mol ppm	y(H <sub>2</sub> S) in mol ppm	X(O <sub>2</sub> ) in %
200 °C	100	100	<3	≈140	100
150 °C	100	98	≈30	≈90	10.6

initial step COS adsorbs on at least one Pd atom followed by dissociation into CO and S adsorbates as described by eqn (5) and (6).<sup>17,19,26–29</sup> Obviously, the coverage of the Pd sites by S grows at lower temperatures (120 °C) thus suppressing the H<sub>2</sub>–O<sub>2</sub> conversion as found in the experiments (Fig. 2 and 4). However, when re-increasing the temperature (>150 °C) the S adsorbates increasingly react with H<sub>2</sub> to yield Pd and H<sub>2</sub>S,<sup>21</sup> which was detected in the gas-phase (eqn (7)). Consequently, the active Pd sites are regenerated and are again available in sufficient abundance for the conversion of O<sub>2</sub> as evidenced in Fig. 4.<sup>14,17,28</sup> Since this reaction is highly exothermic (eqn (3)), it probably leads to a self-acceleration of the reaction rate. This explains the rapid rise of the conversion to over 95% when heating up from 120 °C. Above that, the conversion rises slowly, but can be accelerated by increasing the temperature.



On the other hand, the complete inhibition of the hydrogen–oxygen reaction upon cooling from 200 to 120 °C is also fast within a narrow temperature window. Hence, it can be concluded that at temperatures below 200 °C the formation of elemental sulfur from COS or CS<sub>2</sub> decomposition is faster than its reaction with hydrogen. The continuous chemisorption of sulfur on active Pd sites leads to decreasing levels of oxygen conversion which initiates further cooling of the catalyst internally and therefore increases chemisorption of sites with sulfur even more.

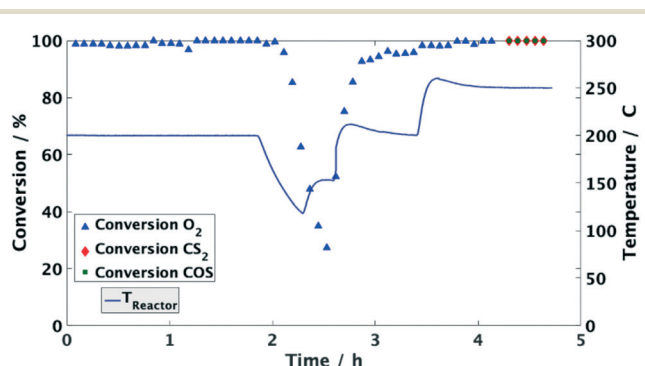


**Fig. 4** Conversion of O<sub>2</sub> and inlet temperature over time using a Pd/Al<sub>2</sub>O<sub>3</sub> catalyst. 3000 1/h, 125 mol ppm COS, 125 mol ppm CS<sub>2</sub>, 50 vol% H<sub>2</sub>, 20 vol% CH<sub>4</sub>, 1 vol% O<sub>2</sub>, N<sub>2</sub> balance. Decrease and increase of O<sub>2</sub> conversion upon change in reaction temperature.

As shown by other groups, the supports' acidity has a positive effect on the regeneration of the catalyst: firstly, the number of active sites is increased because of stabilization of small noble metal particles.<sup>17,28</sup> Secondly, acid support material weakens the Pt–S bond and therefore promotes the formation vacant sites.<sup>30,31</sup>

In this series of experiments no other side reactions were observed. However, it was previously described that metals of group 10 can catalyze the methanation reaction in this temperature range.<sup>33</sup>

### 3.2. Mechanistic studies

*In situ* DRIFTS measurements were conducted with both Pd/Al<sub>2</sub>O<sub>3</sub> as well as Al<sub>2</sub>O<sub>3</sub> to evaluate the role of sulfur in the inhibition of the O<sub>2</sub> conversion at low temperatures. In these studies, COS was taken, as it represents the most prominent organic sulfur compound present in real coke oven gas.<sup>32</sup> The DRIFTS studies were conducted by subsequently exposing the sample to O<sub>2</sub>, H<sub>2</sub> and COS as well as by simultaneously supplying the gases.

**3.2.1. Successive exposure to COS, H<sub>2</sub> and O<sub>2</sub>.** The DRIFT spectra of Pd/Al<sub>2</sub>O<sub>3</sub> recorded after COS exposure at 40 °C exhibit predominant bands in the range between 1200 cm<sup>–1</sup> and 1700 cm<sup>–1</sup> (Fig. 5). Features at 1658 (v<sub>as</sub>(CO<sub>2</sub>)) and 1435 cm<sup>–1</sup> (v<sub>s</sub>(CO<sub>2</sub>)) are associated with HCO<sub>3</sub><sup>–</sup> surface species present on Al<sub>2</sub>O<sub>3</sub>.<sup>34</sup> Furthermore, the bands at 1578 (v<sub>as</sub>(OCS)) and 1330 cm<sup>–1</sup> (v<sub>s</sub>(OCS)) are assigned to HSCO<sub>2</sub><sup>–</sup> coordinated to Al<sub>2</sub>O<sub>3</sub>. The weak bands located at 2050 and 2070 cm<sup>–1</sup> are referred to molecularly adsorbed COS,<sup>35,36</sup> while the weak feature at 2586 cm<sup>–1</sup> is ascribed to the stretching vibration of

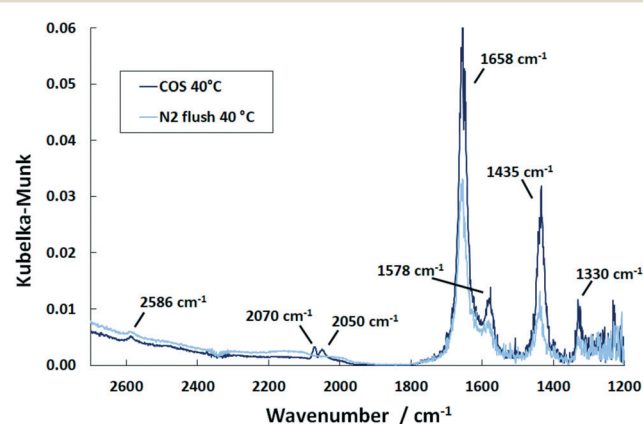


**Fig. 5** DRIFT spectra of the Pd/Al<sub>2</sub>O<sub>3</sub> catalyst after saturation with COS at 40 °C and upon subsequent flushing with N<sub>2</sub> (500 ml min<sup>–1</sup>, 500 ppm COS, N<sub>2</sub> balance).



HS species.<sup>37,38</sup> Since reference tests with pure  $\text{Al}_2\text{O}_3$  provided the same DRIFTS bands, all features are assigned to the chemisorption of COS on the  $\text{Al}_2\text{O}_3$  support. OH stretching bands of the support appear and increase over time in the range from 2700 to 3700  $\text{cm}^{-1}$ . Subsequent flushing with nitrogen leads to disappearance of the band referred to molecularly adsorbed COS and to a slight decrease in the feature of  $\text{HCO}_3^-$  associated with desorption. During the entire time a small and decreasing amount of  $\text{CO}_2$  is detected by MS in the outlet stream.

In the COS exposure at the reaction temperature of 150  $^\circ\text{C}$  (Fig. 6), the DRIFT spectra of the Pd/ $\text{Al}_2\text{O}_3$  catalyst also show the features of  $\text{HCO}_3^-$  and  $\text{HSCO}_2^-$ . However, the intensities of the  $\text{HCO}_3^-$  band decline with time, whereas that of the  $\text{HSCO}_2^-$  entities increase. Also, molecularly adsorbed COS and the HS surface species are again observed. This result is in contrast to Jackson *et al.*<sup>39</sup> who did not observe COS adsorption on Pt/ $\text{Al}_2\text{O}_3$ . Nevertheless, since  $\text{Al}_2\text{O}_3$  is used as a catalyst for the hydrolysis of COS in Claus plants, the mechanism was widely investigated.<sup>25,40</sup> It is generally accepted that in the initial step COS adsorbs on a  $\text{OH}^-$  surface group of  $\text{Al}_2\text{O}_3$  leading to the formation of  $\text{HSCO}_2^-$ . According to George,<sup>41</sup>  $\text{HSCO}_2^-$  further reacts with water, originated from surface OH groups and H present on Pd, and subsequently dissociates to  $\text{CO}_2$ ,  $\text{H}_2\text{O}$  and  $\text{SH}^-$ . Finally,  $\text{SH}^-$  is converted with  $\text{H}_2\text{O}$  into  $\text{H}_2\text{S}$  while  $\text{OH}^-$  is reformed. This mechanism explains the formation of  $\text{HCO}_3^-$  on the surface, which increases at 40  $^\circ\text{C}$ . Since at this temperature only traces are detected by MS, most  $\text{CO}_2$  formed is adsorbed on the surface as indicated by the DRIFTS features at 1658 and 1435  $\text{cm}^{-1}$  (Fig. 5). The decreasing peak at 150  $^\circ\text{C}$  (Fig. 6) shows that  $\text{HCO}_3^-$  is decomposed at higher temperatures and  $\text{CO}_2$  is released to the gas phase. Contrary,  $\text{SH}^-$  remains on the catalyst surface, which is shown by the band located at 2586  $\text{cm}^{-1}$  ( $\nu(\text{HS})$ ), (not shown in Fig. 6).

In contrast to 40  $^\circ\text{C}$ , a double band with maxima at 1890 and 1810  $\text{cm}^{-1}$  is obtained upon COS exposure at 150  $^\circ\text{C}$ . According to the literature,<sup>42,43</sup> the band at 1890  $\text{cm}^{-1}$  refers

to bridged  $\text{Pd}_x\text{-CO}$  (with  $x = 2-3$ ) moieties, whereas the feature at 1810  $\text{cm}^{-1}$  is likely due to threefold hollow binding CO ( $\text{Pd}_3\text{-CO}$ ).<sup>42,44-47</sup> The presence of CO adsorbates is ascribed to the dissociation of COS on Pd sites in line with the literature.<sup>39</sup> However, the proof of resulting Pd-S species is difficult, as the corresponding stretching vibration is expected below 600  $\text{cm}^{-1}$ ,<sup>48</sup> which is not accessible by the DRIFTS cell used.

Compared to 40  $^\circ\text{C}$  a higher partial pressure of  $\text{CO}_2$  is detected in the outlet stream at 150  $^\circ\text{C}$  decreasing over time (Fig. 7). This effect is referred to the above mentioned  $\text{HCO}_3^-$  decomposition. Additionally, it is likely that the adsorbed CO reacts with surface oxygen of the support to yield  $\text{CO}_2$  which is released in the gas phase. When the excessive oxygen is consumed, CO remains on Pd as demonstrated by the growing DRIFTS bands between 1800 and 2000  $\text{cm}^{-1}$  (Fig. 6). This leads to increased absorption of COS on the support (growing bands at 1578 and 1330  $\text{cm}^{-1}$  in Fig. 6). Flushing the catalyst afterwards with nitrogen leads stable adsorbates. However, it has little influence on the  $\text{HCO}_3^-$  and  $\text{HSCO}_2^-$  deposits. The weakly adsorbed COS is removed immediately from the catalyst surface upon  $\text{N}_2$  flushing.

The COS adsorption on bare  $\text{Al}_2\text{O}_3$  performed at 150  $^\circ\text{C}$  provides no CO bands indicating that Pd is necessary for COS dissociation. Besides that, all the other features appear which confirms that they are surface species formed on  $\text{Al}_2\text{O}_3$  and not on the active sites of the catalyst (Fig. 8).

When supplying  $\text{H}_2$  to the catalyst at 150  $^\circ\text{C}$  after COS adsorption and  $\text{N}_2$  flushing all the DRIFTS bands decrease and disappear with the exception of the feature of the  $\text{HCO}_3^-$  species (Fig. 9). Considering the outlet stream, the MS trace showed strong release of water upon addition of  $\text{H}_2$  referred to the reaction with some surface oxygen species of the support.<sup>49</sup> Simultaneously, the MS signal with  $m/z = 32$  increased sharply followed by slow decay (inlay in Fig. 9). Since no oxygen has been added, it is presumably  $^{32}\text{S}$  derived from small amounts of  $\text{H}_2\text{S}$  which were removed from the catalyst by reduction of sulfur species. This is confirmed by small and noisy signals of mass 33 and 34 that were also detected. Since the catalyst reveals little load of Pd (0.3 wt%),

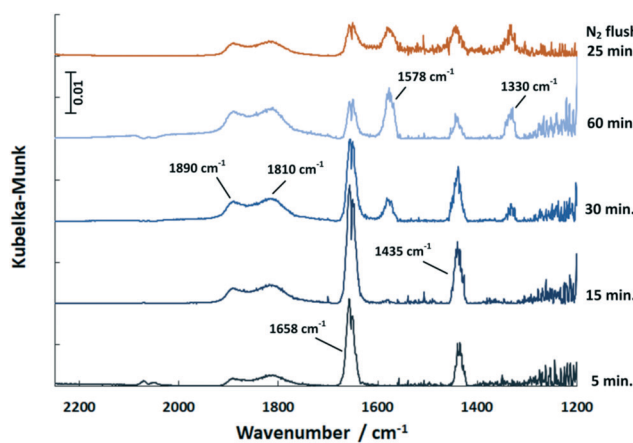


Fig. 6 DRIFT spectra of the Pd/ $\text{Al}_2\text{O}_3$  catalyst exposed to COS at 150  $^\circ\text{C}$  over time and upon subsequent flushing with  $\text{N}_2$  (500  $\text{ml min}^{-1}$ , 500 ppm COS,  $\text{N}_2$  balance).

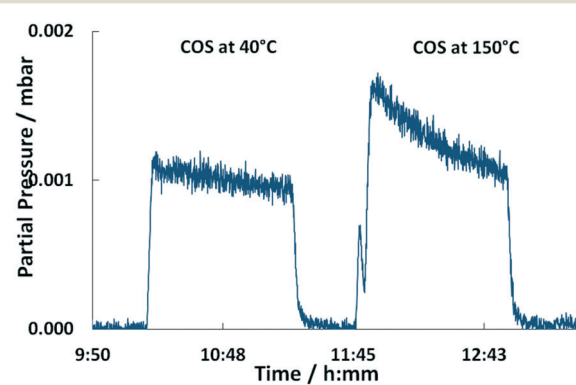


Fig. 7 MS traces of  $m/z = 44$  upon COS exposure of the Pd/ $\text{Al}_2\text{O}_3$  catalyst at 40  $^\circ\text{C}$  and 150  $^\circ\text{C}$  over time (500  $\text{ml min}^{-1}$ , 500 ppm COS,  $\text{N}_2$  balance).

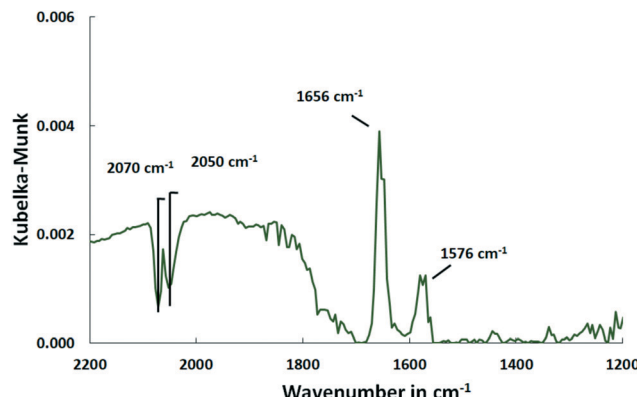


Fig. 8 DRIFT spectra of the  $\text{Al}_2\text{O}_3$  support after saturation with COS at  $150\text{ }^\circ\text{C}$  ( $500\text{ ml min}^{-1}$ ,  $500\text{ ppm COS, N}_2$  balance).

the amount of  $\text{H}_2\text{S}$  is expected to be very small and hence hard to detect.

During the addition of  $\text{H}_2$  the bands in the region above  $3000\text{ cm}^{-1}$  correlated to stretching vibrations of OH groups increase in intensity (Fig. 9), which is associated with the adsorption of  $\text{H}_2\text{O}$ . Additionally, the formation of  $\text{H}_2\text{O}$  enhances the hydrolysis of COS leading to the reaction of  $\text{SH}^-$  and  $\text{H}_2\text{S}$ , respectively. This is confirmed by detection of mass 32 that appears due to ionization and decomposition of COS into CO and S inside the mass spectrometer. Mass 60, that would indicate appearance of COS in the outlet stream was not detected. As shown in Fig. 9, the addition of  $\text{H}_2$  to the catalyst led to further but not complete reduction of the CO peak(s). It is presumed that it is thermally desorbed due to the exothermic reaction of  $\text{H}_2$  with surface oxygen species (eqn (3)). Flushing with  $\text{N}_2$  had no effect on the CO bands.

Continuing with 1 vol%  $\text{O}_2$  after exposure of the catalyst with COS and  $\text{H}_2$  induced a slow but almost complete removal

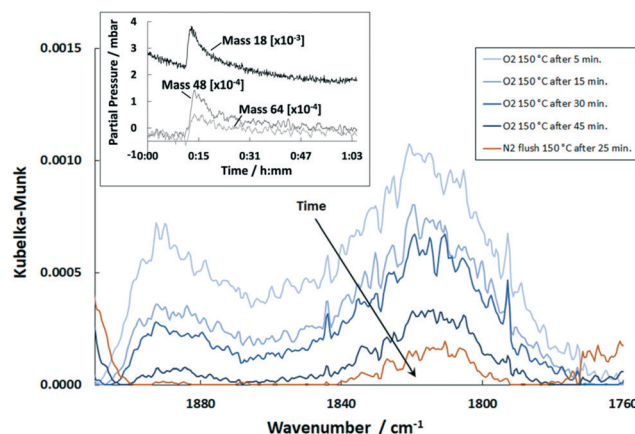


Fig. 10 DRIFT spectra of the  $\text{Pd}/\text{Al}_2\text{O}_3$  catalyst exposed to  $\text{O}_2$  at  $150\text{ }^\circ\text{C}$  over time and upon subsequent flushing with  $\text{N}_2$  ( $500\text{ ml min}^{-1}$ , 1 vol%  $\text{O}_2$ ,  $\text{N}_2$  balance). Inlay shows the simultaneous MS trace of  $m/z = 18$ ,  $m/z = 48$  and  $m/z = 64$ .

of CO (Fig. 10). A small band of threefold bound CO was still observed at  $1807\text{ cm}^{-1}$  after 45 min. Additionally, MS indicates signals with  $m/z$  ratios of 33 and 34, which are clearly more pronounced as compared to the natural abundance of  $^{16}\text{O}^{17}\text{O}$  and  $^{17}\text{O}_2$ . Due to the relatively high partial pressure these masses are unlikely to be  $\text{HS}^-$  or  $\text{H}_2\text{S}$ . Instead they are probably different combinations of H and O atoms and hence of a minor importance of the catalytic activity.

Furthermore, the exposure of  $\text{O}_2$  lead to weak MS peaks 64 ( $\text{SO}_2^+$ ) and 48 ( $\text{SO}^+$ ) associated with  $\text{SO}_2$  (inlay in Fig. 10). Hence, residues of sulfur were still present on the catalyst surface after  $\text{H}_2$  treatment. Since  $\text{SO}_2$  is produced on  $\text{Pd}/\text{Al}_2\text{O}_3$  and  $\text{Al}_2\text{O}_3$ , it can be assumed that remaining sulfur existed on the  $\text{Al}_2\text{O}_3$  support.<sup>50,51</sup> It was shown by Hoyos *et al.*<sup>52</sup> that  $\text{H}_2\text{S}$  adsorbed on  $\text{Al}_2\text{O}_3$  can be completely

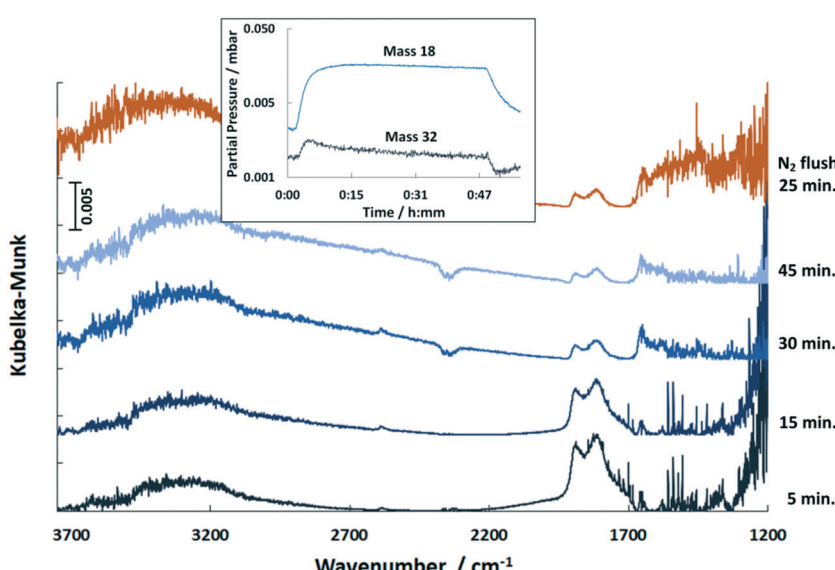


Fig. 9 DRIFT spectra of the  $\text{Pd}/\text{Al}_2\text{O}_3$  catalyst exposed to  $\text{H}_2$  at  $150\text{ }^\circ\text{C}$  over time and upon subsequent flushing with  $\text{N}_2$  ( $500\text{ ml min}^{-1}$ , 60 vol%  $\text{H}_2$ ,  $\text{N}_2$  balance). Inlay shows the simultaneous MS traces of  $m/z = 18$  and  $m/z = 32$ .



oxidized to  $\text{SO}_2$  or  $\text{SO}_3$ . Furthermore, Ordóñez *et al.*<sup>53</sup> showed little desorption of  $\text{SO}_2$  below 200 °C when conducting temperature programmed oxidation of  $\text{SO}_2$ -poisoned  $\text{Pd}/\text{Al}_2\text{O}_3$ . Hence, it is derived that although  $\text{H}_2$  was shown to release sulfur from the support material, residues still remain on  $\text{Al}_2\text{O}_3$  subsequently oxidized by  $\text{O}_2$  to produce  $\text{SO}_2$ . Additionally, the MS signal with  $m/z = 18$  ( $\text{H}_2\text{O}$ ) increased sharply upon exposure to  $\text{O}_2$  and decreased afterwards (inlay in Fig. 10). This indicates that adsorbed hydrogen is still present on the Pd sites even after  $\text{N}_2$  flushing which reacts with  $\text{O}_2$  to form  $\text{H}_2\text{O}$ .<sup>54</sup>

**3.2.2. Simultaneous exposure to COS,  $\text{H}_2$  and  $\text{O}_2$  to  $\text{Pd}/\text{Al}_2\text{O}_3$  or  $\text{Al}_2\text{O}_3$ .** In another DRIFTS investigation, COS,  $\text{H}_2$  and  $\text{O}_2$  were simultaneously fed to mimic practical reaction conditions, whereas the temperature of the catalyst was set to 150 °C (Fig. 11). This approach led to an initial but weak formation of  $\text{HCO}_3^-$  within the first 5 min, continued by a decrease over the remaining 120 min until only a small peak at 1658  $\text{cm}^{-1}$  remained. The previously identified CO peak on Pd (bridged  $\text{Pd}_x\text{-CO}$  (with  $x = 2\text{-}3$  moieties) appeared as a shoulder at around 1866  $\text{cm}^{-1}$ . Reference experiments made with the bare  $\text{Al}_2\text{O}_3$  support basically shows very similar DRIFT spectra with exception of the CO shoulder, which again only appeared with Pd present (Fig. 12).

Considering that the catalyst is plain and active sites are free until the gas mixture is exposed to it, it can be assumed that initially all substances bind to it. Hence, besides the formation of CO-Pd and S-Pd by dissociation of COS, it is likely that oxygen and hydrogen also chemisorb to Pd.<sup>54</sup> Consequently, CO can be oxidized in a Langmuir-Hinshelwood mechanism to  $\text{CO}_2$  and in addition  $\text{H}_2\text{O}$  is formed. The initial increase of  $\text{HCO}_3^-$  bands indicate an adsorption of  $\text{CO}_2$  on  $\text{Al}_2\text{O}_3$ . At the same time,  $\text{CO}_2$  is detected in the MS with a decreasing trend that coincides with the removal of  $\text{HCO}_3^-$  deposits. Therefore, the adsorption is an intermediate phenomenon. In addition, the MS data show a peak of  $\text{H}_2\text{O}$  in the beginning of the experiment, hence a release into the gas phase, that is more pronounced with Pd present. This is plausible, since Pd enhances the oxygen–hydrogen reaction.

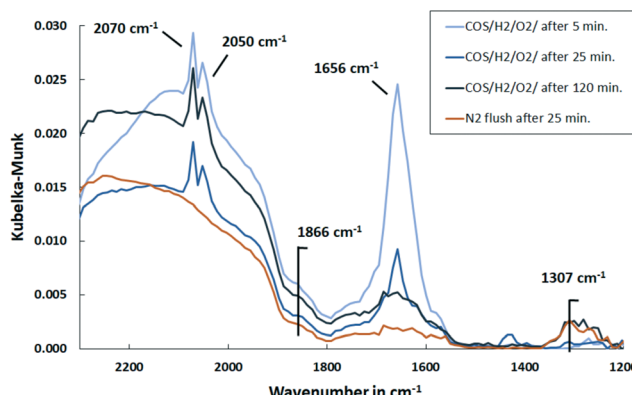


Fig. 11 DRIFT spectra of  $\text{Pd}/\text{Al}_2\text{O}_3$  support exposed to synthetic coke oven gas at 150 °C over time and upon subsequent flushing with  $\text{N}_2$  (500  $\text{ml min}^{-1}$ , 500 ppm COS, 60 vol%  $\text{H}_2$ , 1 vol%  $\text{O}_2$ ,  $\text{N}_2$  balance).

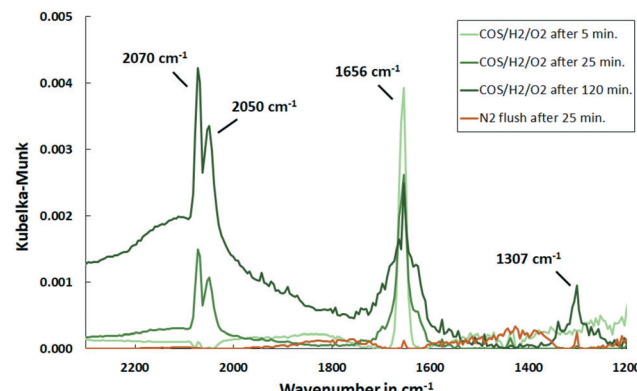


Fig. 12 DRIFT spectra of  $\text{Al}_2\text{O}_3$  support exposed to synthetic coke oven gas at 150 °C over time and upon subsequent flushing with  $\text{N}_2$  (500  $\text{ml min}^{-1}$ , 500 ppm COS, 60 vol%  $\text{H}_2$ , 1 vol%  $\text{O}_2$ ,  $\text{N}_2$  balance).

At 150 °C CO is favorably adsorbed over  $\text{O}_2$ , so in the steady state Pd is preferably covered with CO and S, which inhibits  $\text{O}_2$  adsorption and hence  $\text{CO}_2$  formation. As investigated by Klauck *et al.*<sup>55</sup> and also shown in this work, for the same reason, the oxygen–hydrogen reaction is inhibited.

Since CO-Pd is formed by dissociation of COS, it can be once more assumed that in addition S-Pd is formed. While a high concentration of  $\text{H}_2$  is present in the gas stream, it can be concluded that this bound sulfur reacts with dissociatively adsorbed  $\text{H}_2$  on Pd to  $\text{H}_2\text{S}$  and is removed from the surface.<sup>17</sup> It was previously described that this reduction of metal sulfides such as Pd-S is catalyzed by the adsorption of  $\text{H}_2$  molecules on Pd and their subsequent dissociation into atoms.<sup>17,21</sup>

The conversion of COS to  $\text{H}_2\text{S}$  catalyzed by Pd is confirmed by the MS spectra. A comparison of the outlet streams of simultaneous gas exposure on the catalyst and the support shows that with  $\text{Pd}/\text{Al}_2\text{O}_3$  the partial pressure of mass 60 (COS) is lower (Fig. 13). In addition, comparing the spectra reveals that the masses 34, 33 and 32 showed steady signals in both cases, but with  $\text{Pd}/\text{Al}_2\text{O}_3$  the partial pressure is higher compared to the support only. This indicates the formation of  $\text{H}_2\text{S}$ ,  $\text{HS}^-$  and  $^{32}\text{S}$ , the latter derived from splitting of  $\text{H}_2\text{S}$  in the MS.

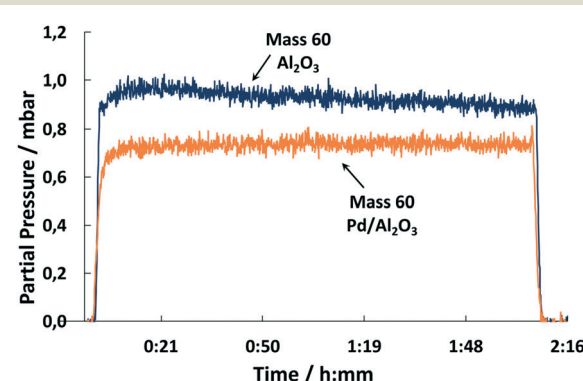


Fig. 13 MS trace of  $m/z = 60$  upon exposure of  $\text{Pd}/\text{Al}_2\text{O}_3$  and  $\text{Al}_2\text{O}_3$  to synthetic coke oven gas (150 °C, 500  $\text{ml min}^{-1}$ , 500 ppm COS, 60 vol%  $\text{H}_2$ , 1 vol%  $\text{O}_2$ ,  $\text{N}_2$  balance).



Moreover, the DRIFT spectra show that CO is bound to Pd over the entire duration. Therefore, it can be concluded that COS adsorption is not inhibited by CO, sulfur or H<sub>2</sub>, hence all four can adsorb on the active sites under these conditions.

Furthermore, HCSO<sub>2</sub><sup>-</sup> appeared as a shoulder in the DRIFT spectra at 1578 cm<sup>-1</sup> only in the beginning and exhibits a lower amount compared to initial COS dosing. This indicates that it is removed by hydrogen as shown before (Fig. 9). Moreover, a small feature at 1307 cm<sup>-1</sup> was detected that increased with time and showed a smaller intensity with Pd present. A peak in that range was previously assigned to be physisorbed or chemisorbed SO<sub>2</sub> on Al<sub>2</sub>O<sub>3</sub>.<sup>50,56</sup> This accumulation of sulfates on Al<sub>2</sub>O<sub>3</sub> were smaller when Pd is present. It was explained by Luo *et al.*<sup>21</sup> that sulfates in proximity to noble metal particles are reduced stepwise to H<sub>2</sub>S by activated H<sub>2</sub> and are subsequently released. This reduction is temperature dependent, since higher temperatures increase the mobility of absorbed sulfates to the region where reduction is possible.

Again, small and noisy signals of mass 64 and 48 were detected with both catalyst and support present. This confirms the formation of SO<sub>2</sub>. However, over time the signals decreased, which leads to the assumption that in the steady state H<sub>2</sub>S is the predominant sulfur species that is released into the gas phase. It is assumed that this again originates in the inhibited adsorption and therefore reactivity of oxygen molecules. In addition, COS molecularly adsorbed on Al<sub>2</sub>O<sub>3</sub> was present that was again instantly removed by flushing with N<sub>2</sub>.

## 4. Conclusions

The performance of a Pd/Al<sub>2</sub>O<sub>3</sub> catalyst was evaluated for the simultaneous hydrogenation of organosulfur compounds and conversion of O<sub>2</sub>, while some mechanistic investigations were made by DRIFT spectroscopy coupled with MS. The catalyst was tested between 120 and 250 °C in a model coke oven gas consisting of H<sub>2</sub>, CH<sub>4</sub>, O<sub>2</sub>, COS and CS<sub>2</sub>. The results showed that at 200 °C and above the organosulfur compounds are almost completely converted to H<sub>2</sub>S. Simultaneously, O<sub>2</sub> entirely reacted with H<sub>2</sub> to H<sub>2</sub>O. Upon lowering the reactor temperature below a critical point, the O<sub>2</sub> conversion is strongly inhibited, whereas COS and CS<sub>2</sub> are still completely converted. Also, the selectivity towards H<sub>2</sub>S is decreased and CH<sub>3</sub>SH appears as additional product. This altered performance is rapidly reversed by increasing the temperature just to 200 and 250 °C, respectively.

The mechanistic examinations of the Pd/Al<sub>2</sub>O<sub>3</sub> catalyst as well as the bare Al<sub>2</sub>O<sub>3</sub> support were conducted by (I) successive gas dosage of COS, H<sub>2</sub> and O<sub>2</sub> and (II) simultaneous exposure to all the reactive gases at 150 °C. It was shown that COS dissociates on the Pd sites to form CO and S adsorbates. These surface species located on the Pd sites prevent the adsorption of O<sub>2</sub> and they therefore strongly inhibit the oxygen–hydrogen reaction as observed in the catalytic performance tests. In addition, it was demonstrated

that CO was removed from Pd due to displacement at 150 °C and it is assumed that desorption is accelerated at higher temperatures. Furthermore, the presence of H<sub>2</sub> leads to a removal of bound sulfur to H<sub>2</sub>S.

Moreover, it was shown that COS also adsorbs on the Al<sub>2</sub>O<sub>3</sub> support resulting in the formation of HSCO<sub>2</sub><sup>-</sup>. Subsequently, HSCO<sub>2</sub><sup>-</sup> reacts with OH<sup>-</sup> surface groups to CO<sub>2</sub> and H<sub>2</sub>S, which can re-adsorb to yield HCO<sub>3</sub><sup>-</sup> species. However, HSCO<sub>2</sub><sup>-</sup> plays a rather minor role in the conversion of COS to H<sub>2</sub>S.

To conclude, the strong blockage of the catalytically active Pd sites by CO and S inhibits side reactions. It is reversible by two effects: firstly, the increase of temperature that leads to the desorption of CO and secondly, by the presence of H<sub>2</sub> in the feed stream that removes bound sulfur to form H<sub>2</sub>S.

Finally, this study shows that commercially available Pd/Al<sub>2</sub>O<sub>3</sub> catalysts can be effectively taken for the removal of organosulfur compounds and oxygen from coke oven model gas. Also, the high amount of H<sub>2</sub> simply facilitates the catalyst regeneration. Consequently, HDS by Pd/Al<sub>2</sub>O<sub>3</sub> catalysts is considered as a suitable method for the deep desulfurization of coke oven gas to supply synthesis gas for the chemical industry.

## Conflicts of interest

There are no conflicts to declare.

## References

- 1 C. Song, *Catal. Today*, 2003, **86**, 211–263.
- 2 C. Song and X. Ma, *Appl. Catal., B*, 2003, **41**, 207–238.
- 3 C. Peng, R. Guo and X.-C. Fang, *Catal. Lett.*, 2016, **146**, 701–709.
- 4 N. Azizi, S. A. Ali, K. Alhooshani, T. Kim, Y. Lee, J.-I. Park, J. Miyawaki, S.-H. Yoon and I. Mochida, *Fuel Process. Technol.*, 2013, **109**, 172–178.
- 5 F. Rashidi, T. Sasaki, A. M. Rashidi, A. Nemati Kharat and K. Jozani, *J. Catal.*, 2013, **299**, 321–335.
- 6 X. Fang, R. Guo and C. Yang, *Chin. J. Catal.*, 2013, **34**, 130–139.
- 7 F. Sowa, B. Otten, J. Kamp and E. Profase, *Proceedings of ICC*, Ranchi, India, 2009, 20–22 January 2009 (2009), pp. 148–170.
- 8 H. Hiller, R. Reimert and H.-M. Stönnier, *Ullmann's Encyclopedia of Industrial Chemistry*, 2000, pp. 403–421.
- 9 G. C. A. Schuit and B. C. Gates, *AIChE J.*, 1973, **19**, 417–438.
- 10 E. Furimsky and F. E. Massoth, *Catal. Today*, 1999, **52**, 381–495.
- 11 *Catalysis*, ed. J. R. Anderson and M. Boudart, Springer, Berlin Heidelberg, Berlin, Heidelberg, 1996.
- 12 W. Boll, G. Hochgesand, C. Higman, E. Supp, P. Kalteier, W.-D. Müller, M. Kriebel, H. Schlichting and H. Tanz, *Ullmann's Encyclopedia of Industrial Chemistry*, 2000, pp. 483–539.
- 13 H. R. Reinhoudt, R. Troost, A. D. van Langeveld, S. T. Sie, J. van Veen and J. A. Moulijn, *Fuel Process. Technol.*, 1999, **61**, 133–147.



14 H. R. Reinhoudt, R. Troost, S. van Schalkwijk, A. D. van Langeveld, S. T. Sie, J. van Veen and J. A. Moulijn, *Fuel Process. Technol.*, 1999, **61**, 117–131.

15 E. W. Qian, K. Otani, L. Li, A. Ishihara and T. Kabe, *J. Catal.*, 2004, **221**, 294–301.

16 A. Ishihara, F. Dumeignil, J. Lee, K. Mitsuhashi, E. W. Qian and T. Kabe, *Appl. Catal., A*, 2005, **289**, 163–173.

17 J.-F. Chiou, Y.-L. Huang, T.-B. Lin and J.-R. Chang, *Ind. Eng. Chem. Res.*, 1995, **34**, 4277–4283.

18 B. Vogelaar, *Appl. Catal., A*, 2003, **251**, 85–92.

19 C. H. Bartholomew, P. K. Agrawal and J. R. Katzer, *Adv. Catal.*, 1982, 135–242.

20 C. H. Amberg, *J. Less-Common Met.*, 1974, **36**, 339–352.

21 J.-Y. Luo, D. Kisinger, A. Abedi and W. S. Epling, *Appl. Catal., A*, 2010, **383**, 182–191.

22 N. S. Fígoli and P. C. L'Argentiere, *J. Mol. Catal. A: Chem.*, 1997, **122**, 141–146.

23 G. Emig and E. Klemm, *Technische Chemie: Einführung in die Chemische Reaktionstechnik*, 5., aktualisierte und erg. Aufl., Springer, Berlin [u.a.], 2005.

24 P. Clark, N. I. Dowling and M. Huang, *Proceedings of Brimstone Sulfur Symposium*, Vail, Colorado, USA, September 10–14th, 2012, pp. 16–37.

25 C. Rhodes, S. A. Riddel, J. West, B. Williams and G. J. Hutchings, *Catal. Today*, 2000, **59**, 443–464.

26 D. L. Mowery and R. L. McCormick, *Appl. Catal., B*, 2001, **34**, 287–297.

27 C. H. Bartholomew, *Catalyst Deactivation*, 2001, **212**, 17–60.

28 P. Albers, J. Pietsch and S. F. Parker, *J. Mol. Catal. A: Chem.*, 2001, **173**, 275–286.

29 T. Yu, *Appl. Catal., B*, 1998, **18**, 105–114.

30 J. T. Miller and D. C. Koningsberger, *J. Catal.*, 1996, **162**, 209–219.

31 B. H. Cooper and B. B. Donnis, *Appl. Catal., A*, 1996, **137**, 203–223.

32 P. Svoronos and T. J. Bruno, *Ind. Eng. Chem. Res.*, 2002, **41**, 5321–5336.

33 G. A. Mills and F. W. Steffgen, *Catal. Rev.: Sci. Eng.*, 2006, **8**, 159–210.

34 E. Laperdrix, I. Justin, G. Costentin, O. Saur, J. Lavalley, A. Aboulayt, J. Ray and C. Nédez, *Appl. Catal., B*, 1998, **17**, 167–173.

35 R. Fiedorow, *J. Catal.*, 1984, **85**, 339–348.

36 K. K. Pandey, *Coord. Chem. Rev.*, 1995, **140**, 37–114.

37 J. Jones, V. Dupont, R. Brydson, D. Fullerton, N. Nasri, A. Ross and A. Westwood, *Catal. Today*, 2003, **81**, 589–601.

38 G. Larsen, E. Lotero, R. D. Parra, L. M. Petkovic, H. S. Silva and S. Raghavan, *Appl. Catal., A*, 1995, **130**, 213–226.

39 S. Jackson, P. Leeming and G. Webb, *J. Catal.*, 1996, **160**, 235–243.

40 J. West, B. P. Williams, N. Young, C. Rhodes and G. J. Hutchings, *Catal. Lett.*, 2001, **74**, 111–114.

41 Z. George, *J. Catal.*, 1974, **35**, 218–224.

42 E. Ozensoy and D. Wayne Goodman, *Phys. Chem. Chem. Phys.*, 2004, **6**, 3765.

43 M. Kantcheva and I. Cayirtepe, *J. Mol. Catal. A: Chem.*, 2006, **247**, 88–98.

44 M. Valden, R. L. Keiski, N. Xiang, J. Pere, J. Aaltonen, M. Pessa, T. Maunula, A. Savimäki, A. Lahti and M. Härkönen, *J. Catal.*, 1996, **161**, 614–625.

45 A. I. Boronin, E. M. Slavinskaya, I. G. Danilova, R. V. Gulyaev, Y. Amosov, P. A. Kuznetsov, I. A. Polukhina, S. V. Koscheev, V. I. Zaikovskii and A. S. Noskov, *Catal. Today*, 2009, **144**, 201–211.

46 G. Rupprechter, H. Unterhalt, M. Morkel, P. Galletto, L. Hu and H.-J. Freund, *Surf. Sci.*, 2002, **502–503**, 109–122.

47 M. Borasio, *Polarization Modulation Infrared Reflection Absorption Spectroscopy on Pd Model Catalysts at Elevated Pressure*, PhD, Freie Universität Berlin, Berlin, 2006.

48 B. Liang, X. Wang and L. Andrews, *J. Phys. Chem. A*, 2009, **113**, 3336–3343.

49 P. Ammendola, P. S. Barbato, L. Lisi, G. Ruoppolo and G. Russo, *Surf. Sci.*, 2011, **605**, 1812–1817.

50 M. S. Wilburn and W. S. Epling, *Appl. Catal., A*, 2017, **206**, 589–598.

51 J. Lampert, M. Kazi and R. Farrauto, *Appl. Catal., B*, 1997, **14**, 211–223.

52 L. J. Hoyos, H. Praliaud and M. Primet, *Appl. Catal., A*, 1993, **98**, 125–138.

53 S. Ordóñez, P. Hurtado and F. V. Díez, *Catal. Lett.*, 2005, **100**, 27–34.

54 W. Reschetilowski, *Einführung in die Heterogene Katalyse*, Springer Berlin Heidelberg, Berlin, Heidelberg, 2015.

55 M. Klauck, E.-A. Reinecke, S. Kelm, N. Meynet, A. Bentaïb and H.-J. Allelein, *Nucl. Eng. Des.*, 2014, **266**, 137–147.

56 E. Laperdrix, A. Sahibed-dine, G. Costentin, O. Saur, M. Bensitel, C. Nédez, A. B. Mohamed Saad and J. C. Lavalley, *Appl. Catal., B*, 2000, **26**, 71–80.

